PCCP

Decoupling between translation and rotation of water in the proximity of a protein molecule

Journal:	*Physical Chemistry Chemical Physics*
Manuscript ID	CP-ART-05-2020-002416.R1
Article Type:	Paper
Date Submitted by the Author:	28-Jun-2020

Complete List of Authors:	Tan, Pan; Shanghai Jiao Tong University, school of physics and astronomy and institute of natural sciences Huang, Juan; Shanghai Jiao Tong University Mamontov, Eugene; Oak Ridge National Laboratory, Spallation Neutron Source Garcia Sakai, Victoria; Rutherford Appleton Laboratory, ISIS Facility Merzel, Franci; National Institute of Chemistry, Liu, Zhuo; Shanghai Jiao Tong University Ye, Yiyang; Shanghai Jiao Tong University Liang, Hong; Shanghai Jiao Tong University,

Decoupling between translation and rotation of water in the proximity of a protein molecule

Pan Tan,[1,2] Juan Huang,[3] Eugene Mamontov,[4] Victoria García Sakai,[5] Franci Merzel,[6] Zhuo Liu,[1,2] Yiyang Ye,[7] Liang Hong[1,2]*

[1]*School of Physics and Astronomy, Shanghai Jiao Tong University, Shanghai 200240, China*

[2]*Institute of Natural Sciences, Shanghai Jiao Tong University, Shanghai 200240, China*

[3]*School of Life Sciences and Biotechnology, Shanghai Jiao Tong University, Shanghai 200240, China*

[4]*Spallation Neutron Source, Oak Ridge National Laboratory, Oak Ridge, Tennessee 37831, USA*

[5]*ISIS Facility, Rutherford Appleton Laboratory, Chilton, Didcot OX11 0QX, UK*

[6]*Theory Department, National Institute of Chemistry, SI 1000 Ljubljana, Slovenia*

[7]*Zhiyuan College, Shanghai Jiao Tong University, Shanghai 200240, China*

Abstract

The interaction between water and bio-macromolecules is of fundamental interest in biophysics, biochemistry and physical chemistry. By combining neutron scattering and molecular dynamics simulations on a perdeuterated protein at a series of hydration levels, we demonstrated that the translational motion of water is slowed down more significantly than its rotation when water molecules approaching the protein molecule. Further analysis of the simulation trajectories reveals that the observed decoupling results from the fact that the translational motion of water is more correlated over space, and more retarded by the charged/polar residues and spatial confinement on the protein surface than the rotation. Moreover, around the stable protein residues (with smaller atomic fluctuations), water exhibits more decoupled dynamics, indicating a connection between the observed translation-rotation decoupling in hydration water and the local stability of the protein molecule.

Introduction

The dynamics of hydration water plays a crucial role in determining the structure, dynamics and function of bio macromolecules[1-7]. Particularly, the diffusive motions of water aids ligand and proton transfer, protein-DNA, protein-ligand recognition, protein dynamic transition and folding of the protein molecule into the correct 3-D structure[7-15], while its rotational motions lubricate the local structural motifs of bio-macromolecule and lower the entropic cost during protein folding[16-18]. A wide range of experimental techniques, including NMR, neutron scattering, dielectric spectroscopy, depolarized light scattering, 2D-infrared spectroscopy, and Terahertz spectroscopy, etc., have been applied to explore the dynamics of hydration water on various bio macromolecules[6, 19-27]. Although most experimental results support a common view that the dynamics of water molecules are slowed down in the proximity of biomolecules, the extent of retardation and the thickness of hydration shell, i.e., number of layers of water molecules being perturbed at the interface, remain highly controversial, as reported by different experimental techniques. NMR measurements suggested that hydration water on the protein surface is slowed down by a factor between 2 to 6 [25, 28, 29] as compared to the bulk water, and an even smaller factor of 1.8 was reported from femtosecond infrared measurements[23]. In contrast, dielectric spectroscopy found ultra-slow motions of protein-surface water, orders of magnitude slower than bulk water[24, 30]. The experimental determination of the thickness of hydration shell is also in active debate. NMR showed that the dynamics of water is

altered only within 3-4 Å around the bio-macromolecules, i.e., a single layer of water molecules[28], while Terahertz spectroscopy indicated that the hydration shell is ~ 20 Å thick, suggesting that more than six layers of water are perturbed on the bio-molecular surface[19, 31]. A possible mechanism to rationalize these contradictions can be inferred from Refs[5, 32, 33] that different experimental techniques probe distinct types of water dynamics, e.g., diffusion, rotation and vibrations, and these modes might be perturbed differently by the bio macromolecule. However, a systematic investigation of such mechanism is lacking.

Herein, by performing quasi-elastic neutron scattering (QENS) experiments on perdeuterated cytochrome P450 (CYP) with well-controlled hydration levels, we found that both the translational and rotational motions of water are slowed down with decreasing the hydration, with the translational mobility decreasing more dramatically. Further molecular dynamics simulations confirmed the experimental finding and found that the retardation effect propagates to the second hydration layer for translation while being primarily restrained in the first layer for rotation. The simulation also revealed that the experimentally observed translation-rotation decoupling results from the fact that the water translation is highly correlative over space and more constrained by spatial confinement and charged/polar residues on the protein surface.

Results and discussion

Neutron spectra derived experimentally and from MD simulation.

To examine the dynamics of hydration water on the protein, we conducted QENS experiments on hydrated perdeuterated CYP at 280 K at four hydration levels (gram H_2O/gram protein), i.e., h = 0.4, 1.0, 2.0 and 4.0. h=0.4 corresponds to a case that the protein surface is covered roughly by a single layer of water molecules[1], while h = 4.0 denotes multi layers of surface water[21] and approximates to that in a real cell[34], thus of most biological relevance. Here, the samples used for neutron experiments are perdeuterated proteins hydrated in H_2O, so that the neutron signal from the protein itself is strongly suppressed, since the incoherent scattering cross section of hydrogen is one order of magnitude larger than the scattering cross sections of other elements[35, 36]. Consequently, the measured neutron data are primarily reflecting the motions of water. Neutron scattering experiments on h = 0.4 and 1.0 samples were performed using the backscattering spectrometer BASIS at Oak Ridge National laboratory in the US[37], while those on h = 2.0 and 4.0 were conducted at the OSIRIS Spectrometer at the ISIS Neutron and Muon Source in UK[38, 39]. To complement the neutron scattering experiment, all-atom molecular dynamics (MD) simulations were performed at the same hydration levels and temperature as the experiments. More detailed information on sample preparation, experimental setup and MD protocols are provided in the SI.

As an example, Fig. 1A presents the experimental and MD-derived neutron susceptibility spectra $\chi''(q, E)$ for water on CYP at h =1.0 at various scattering wave vectors q, in the energy range from 5 to 200 μeV, corresponding to the time window from 5 to 200 ps. Here, $\chi'' = S(q, E)/n_B(E)$, where $S(q, E)$ is the dynamic structure factor, i.e., the distribution of the dynamic modes in the sample over the energy transfer E at a given q (obtained directly from the experiment), and $n_B(E)$ is the Bose factor, $1/[\exp(E/k_BT)-1]$. The experimental and MD-derived neutron spectra for other hydration levels and bulk water are provided in Fig. S1 in the SI. As can be seen, the MD-derived $\chi''(q, E)$ is in good agreement with experiment at all h and q, quantitatively validating the water dynamics seen in MD simulations on the pico-to-nanosecond timescales.

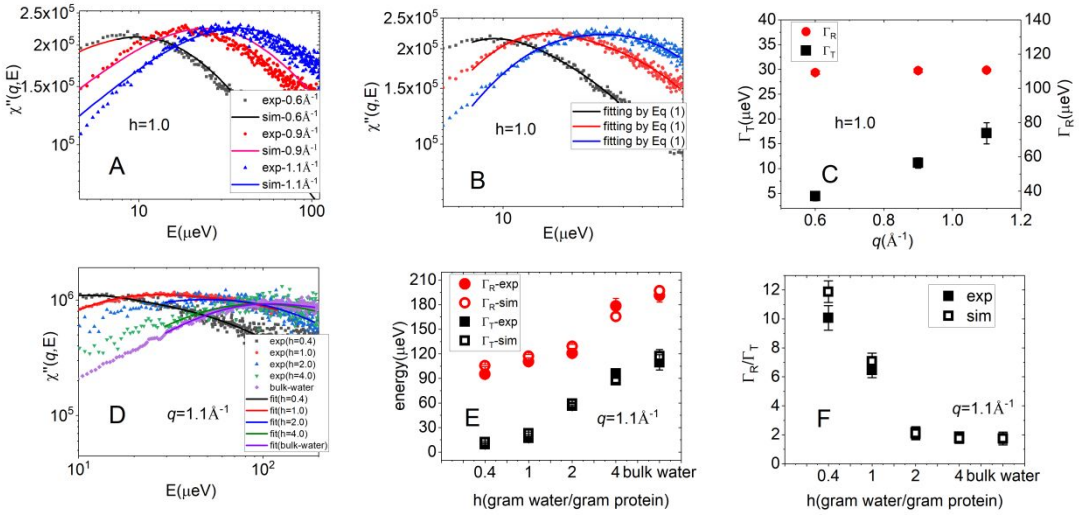

Figure 1. Neutron spectra, $\chi''(q, E)$, of protein-surface water at 280 K. (A) $\chi''(q, E)$ of water molecules derived from experiment and from MD simulation on perdeuterated CYP at different q values, for a hydration level of h = 1.0. (B) $\chi''(q, E)$ and the corresponding fitting curves using the Debye function (Eq. (1)) for h = 1.0 at q=0.6Å^{-1}, 0.9Å^{-1} and 1.1Å^{-1}. (C) The fitting results of Γ_T and Γ_R derived from (B). (D) $\chi''(q, E)$ and the corresponding fitting curves using the Debye function (Eq. (1)) at different h when q=1.1 Å^{-1}. (E) The fitting results of Γ_T and Γ_R derived from the experimental spectra (filled symbols) and from the simulation ones (empty symbols). (F) The ratio of Γ_R/Γ_T derived from (E). The fitting parameters for the experimental neutron spectra measured at different q and h are summarized in Table S1 in SI.

Translational and rotational mobility of hydration water measured experimentally.

The dynamics of water in the pico-to-nanosecond timescale involves both translational and rotational components[22, 40]. To quantitatively characterize these two types of motions, $\chi''(q, E)$ is modeled using the Debye function [21, 40, 41],

$$\chi''(q,E) = e^{-\langle u^2\rangle q^2/3} \otimes \left[A(q) \otimes \frac{\Gamma_T(q)}{E^2 + \Gamma_T^2(q)} + B(q) \otimes \frac{2\Gamma_R(q) + \Gamma_T(q)}{E^2 + [2\Gamma_R(q) + \Gamma_T(q)]^2} \right] \otimes (e^{E/k_BT} - 1) \quad (1)$$

where $e^{-\langle u^2\rangle q^2/3}$ is the Debye-Waller factor, and $\langle u^2\rangle$ represents the mean-squared vibrational amplitude of atoms, assumed to be a constant (0.23Å^2), whose value is taken from ref [42]. Γ_T and Γ_R characterize the translational and rotational mobility, and A and B measure the contributions of the translational and rotational components to the neutron signals. We note that, the choice of the value of $\langle u^2\rangle$ will only affect the absolute value of the weighting factor A and B, but not the ratio of A/B or the value of Γ_T and Γ_R. Fig. 1B presents fittings of Eq. (1) to $\chi''(q, E)$ at h = 1.0 measured at different q, and the resulting Γ_T and Γ_R are displayed in Fig. 1C. As can be seen, Γ_T increases rapidly with q, as Γ_T is inversely proportional to the characteristic time for particles to diffuse a distance of ~ 1/q. For normal (Brownian) diffusion Γ_T is proportional to q^2 and is what is expected for bulk water (see Fig. S1G), however for lower hydrations it can take higher power law (e.g. h=0.4, it is proportional to $q^{2.5}$), characteristic of a sub-diffusive regime[35, 43]. In contrast, Γ_R is independent of

q as rotations are localized motions. These findings are similar to those of Ref[21, 40].

The neutron spectra collected from samples at different hydration levels measured at q=1.1Å^{-1} are presented in Fig. 1D, where the peak in $\chi''(q,E)$ shifts drastically to higher energy with increasing h, indicating that the average mobility of water molecules increases upon hydration. As the spectra measured at q =1.1Å^{-1} display a full peak with both low and high frequency sides exhibited at all hydration levels, ensuring more reliable analysis, the comparison of neutron data at different h is thus mainly conducted at this q in the present work. The analysis of experimental data at other q also yields qualitative similar results.

The Debye function (Eq.(1)) is further applied to model $\chi''(q,E)$ at different h. Fig. 1D presents the fittings conducted at q =1.1Å^{-1} and the resulting Γ_T and Γ_R are displayed in Fig. 1E (filled symbols). Evidently both Γ_T and Γ_R decrease when reducing h, i.e., both the translation and rotation of water molecules are slowed down when decreasing the level of hydration. By close examination, one can find that Γ_T is reduced by one order of magnitude when decreasing h from 4.0 to 0.4, while Γ_R changes only by a factor of 2. Hence, the retardation effect on the translation of water molecules is much more significant than its rotation. As further illustrated by Fig. 1F (filled symbols), the ratio between Γ_R and Γ_T increases from 2 to 10 when changing from a concentrated solution (h=4.0) to a hydrated powder (h=0.4) where the protein molecule is only covered by a single layer of water molecules. It indicates that the translation and rotation are gradually decoupled when the water molecule proceeds toward the protein. Similar conclusions can be also obtained when analyzing the MD-derived neutron spectra (empty symbols in Figs. 1E and 1F).

As a control, we performed a similar analysis on the MD-derived neutron-spectra of bulk water at different temperatures ranging from 280 K to 320 K (Fig. 2A). As seen in Fig. 2B, Γ_T obtained from the fitting is strictly coupled to Γ_R, i.e., the ratio of the two parameters is temperature-independent (Fig. 2C). This is expected for a homogeneous simple liquid where the Stokes-Einstein relation and the Stokes-Einstein-Debye relation are valid[44]. This control analysis implies that the experimentally observed decoupling of the translational and rotational motions of hydration water on the protein surface (Figs. 1E and F) is an intrinsic property of the system studied rather than resulting from the model used for analysis (Eq. (1)).

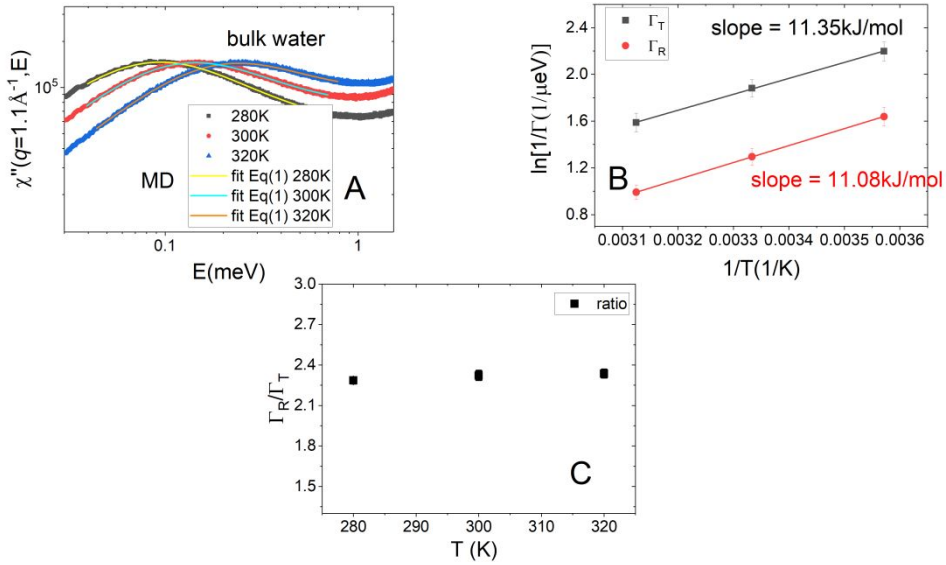

Figure 2. (A) Neutron susceptibility spectra of bulk water derived from MD simulations at different temperatures at q=1.1 Å^{-1}, and the corresponding fitting curves using the Debye function (Eq.(1)).

(B) Temperature dependence of $\ln(1/\Gamma_T)$ and $\ln(1/\Gamma_R)$, where Γ_T and Γ_R are derived by the fittings in (A). Their temperature dependences (the slopes) furnish the corresponding activation energies by assuming an Arrhenius law, which are ~11 kJ/mol for both translational and rotational motions, which is approximately equal to the energy required to break one hydrogen bond. The same energy barrier indicates that Γ_T and Γ_R are coupled when changing temperature. (C) The ratio of Γ_R/Γ_T as a function of temperature.

MD-derived microscopic mechanism for translation-rotation decoupling in hydration water

To acquire a more microscopic description of the observed decoupled dynamics in hydration water, we performed detailed analysis on the MD trajectories of individual water molecules at different hydration levels. To quantitatively characterize the microscopic translational and rotational mobility of water molecules, two quantities are calculated for each water molecule: the residence time, τ_{res}, for it to move a given distance (3.5Å), and the characteristic rotational time, τ_{rot}. Here, 3.5Å is chosen as it is the first minimum in the radial distribution function between oxygen atoms in bulk and hydration water, representing the thickness of water's first coordination shell[5, 35].

To calculate the residence time of water at different hydration levels, including bulk water, the position of the oxygen atom of each water molecule is tracked starting from the beginning of the trajectory, t_0, until the time instant t_1 when it moves a distance of 3.5Å from its position at t_0. Here, the motion from t_0 to t_1 is named as one moving step, and t_1-t_0 is defined as the corresponding residence time, τ_{res}. Then, the time origin is shifted to t_1 to redo the tracking process to identify the second step of 3.5 Å motion for the water molecule and the corresponding τ_{res}. In this way, a series of moving steps for each water molecule can be determined within its entire simulation trajectory, and the mean value of τ_{res} can be obtained by averaging over the number of steps. A further average is applied over all water molecules in the simulation. The results are presented in Fig. 3A, which furnish the average time for all water molecules to move a distance of 3.5Å at a given hydration level or in the bulk water. The so-obtained τ_{res} decreases dramatically by about an order of magnitude from h=0.4 to 4.0, mimicking the hydration dependence of $1/\Gamma_T$ derived from the neutron spectra. Although τ_{res} is defined differently from $1/\Gamma_T$, both parameters are linked closely to the translational mobility of water, which might rationalize their similar hydration dependence.

For the rotational motion, the characteristic time, τ_{rot}, is defined as the time when the rotational autocorrelation function of a water molecule decays to 0.1[44]. This is given by

$$C(t) = \left(P_2 \left[\vec{e}(0) \cdot \vec{e}(t) \right] \right), \tag{2}$$

where P_2 is the second order Legendre polynomial, $\vec{e}(t)$ is the unit vector of the dipole moment of the water molecule at time t, and the parentheses "()" denotes the time average. The mean values of τ_{rot} averaged over all water molecules at different hydration levels are presented in Fig. 3A. The hydration dependence of τ_{rot} is much weaker than τ_{res}, i.e., decoupling between translational and rotational motion. And τ_{rot} exhibits similar hydration dependence as $1/\Gamma_R$.

During a lengthy simulation and at high hydration levels, e.g., h=4.0, a water molecule can transit among different hydration layers on the protein surface. The question then arises as to whether there is a difference in the dynamics of water molecules within different hydration layers. To address this question, one needs to define the hydration layers first. Here, the first hydration layer is defined to include all water molecules whose oxygen atoms are located at a distance of $d \leq$ 3.5 Å from the closest protein atom. The second layer is defined for water molecules whose oxygen

atoms are within a distance of $3.5 < d \leq 7$Å. A similar criteria follows for the 3rd to 5th layers, increasing d by 3.5 Å every time. To analyze τ_{res} of each water molecule within a given hydration layer, its entire MD trajectory is broken into separate time intervals that correspond to the time during which the water molecule stays in one hydration layer. Then, one can easily identify all the time intervals for a given water molecule when it sits at the desired hydration layer. During one of such time intervals, the water molecule can make a specific number of moving steps of 3.5 Å, which can be explicitly identified the same way as described above. (The final moving step of the time interval corresponds to a jump of the water molecule between two adjacent hydration layers, the associated τ_{res} is assigned to the layer where the jump starts.) Then, the mean value of τ_{res} can be obtained by averaging over the number of steps within the time interval. This mean value is further averaged over all the time intervals of the trajectory when the water molecule stays within the layer, and further averaged over all water molecules. The resulting residence time is thus the average time it takes for all water molecules that stay at a given hydration layer to move a distance of 3.5 Å. To characterize the rotational mobility of water in the same layer, τ_{rot}, is calculated using Eq.(2) in the same time interval, and then averaged in a similar way. The so-obtained τ_{res} and τ_{rot} for each hydration layer are presented in Fig. 3B and C, respectively. As can be seen, the translational motion of water is significantly slowed down in both the first and second hydration layers, while the retardation of water rotation is mostly limited within the first layer (Fig. 3C). Moreover, the translational motion in the first hydration layer is retarded by 4 times as compared to the bulk water (Fig. 3B), whereas this factor is less than 2 for rotations (Fig. 3C). The ratio between τ_{res} and τ_{rot}, presented in Fig. 3D, demonstrates that the decoupling between translation and rotation starts at the second hydration layer and is more significant in the first one. In Figs. 3B to D, we have excluded the water molecules trapped in the cavity inside the protein molecule to explicitly analyze the protein-surface water. The same applies to Figs. 4 to 7. A detailed definition of cavity water can be found in section S3.3. in the SI.

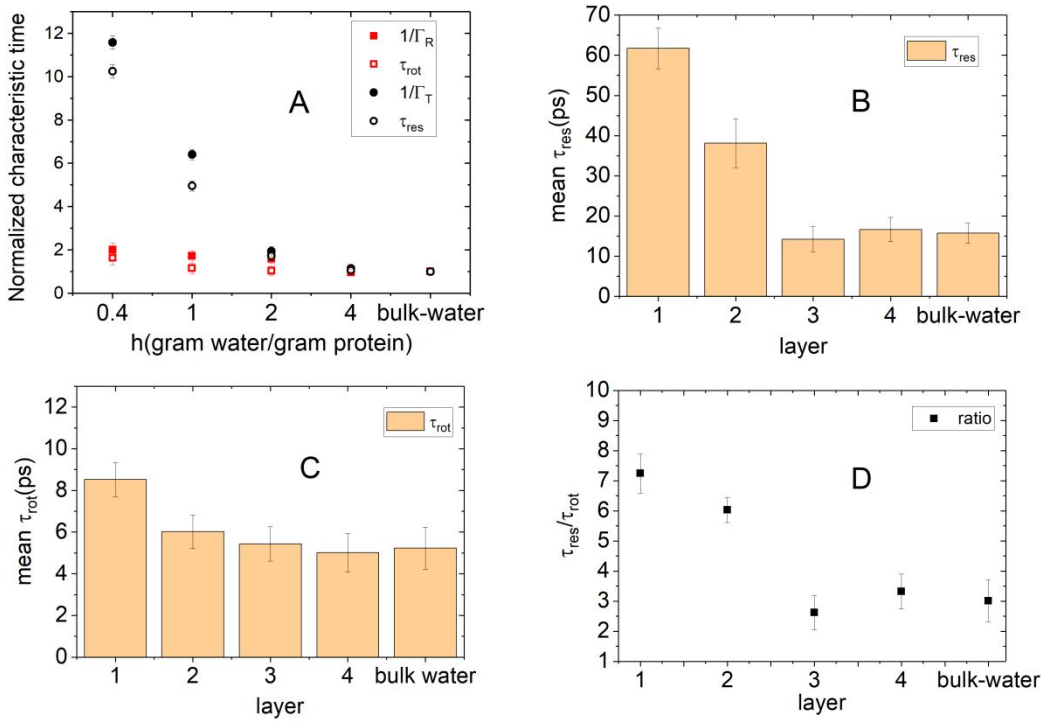

Figure 3. (A) The hydration dependence of $1/\Gamma_T$, $1/\Gamma_R$, τ_{res} and τ_{rot}, normalized by the data for bulk water derived from MD. The values of Γ_T and Γ_R were derived from the MD-derived neutron spectra at q=1.1 Å^{-1} (data were taken from Fig. 1E). MD-derived mean values of (B) τ_{res} and (C) τ_{rot} and (D) their ratio, τ_{res}/τ_{rot}, of water molecules in each hydration layer on the protein surface. The analysis was performed using the system with h=4.0. All the analysis in B to C are based on protein-surface water as the cavity water molecules inside the protein have been excluded (See detailed procedures in SI). The same applies to Fig. 4 to 7.

To explore the effects of the protein surface on the dynamical decoupling in the hydration water, we analyzed the translational and rotational mobility of the water molecules around each surface residue at h=4.0. Briefly, when a water molecule approaches a protein-surface residue, i.e., the distance between the water oxygen and the closest atom in the residue is smaller than 3.5 Å, and stays within that distance for a period of time, this time is denoted as the trapping time of the water molecule around this residue, τ_{trap}. For these 'trapped' water molecules, τ_{rot} can be calculated using Eq.(2) the same way as before during the trapping time. The mean values of τ_{trap} and τ_{rot} are obtained by averaging over all surrounding water molecules and mapped to the residue. As a result, each protein-surface residue has the characteristic values of τ_{trap} and τ_{rot}, characterizing the translational and rotational motilities of the water molecules surrounding it, respectively.

In Fig. 4A and B, we plot the distributions of τ_{trap} and τ_{rot} for water molecules which are mapped to their neighboring protein surface residues, as a function of their distance from the center of mass of the biomolecule. As can be seen, larger τ_{trap} tends to be closer to the center of protein. In contrast, the spatial distribution of τ_{rot} is much more uniform. In Fig. 4C, we highlighted the residues (red region) which constitute the peak in Fig. 4A at ~ 17 Å, around which water molecules exhibit the longest τ_{trap}. These residues are mostly located at the clefs or concave spots on the protein surface. Hence, the translational motion of water is more restrained by the protein-surface confinements as compared to its rotation.

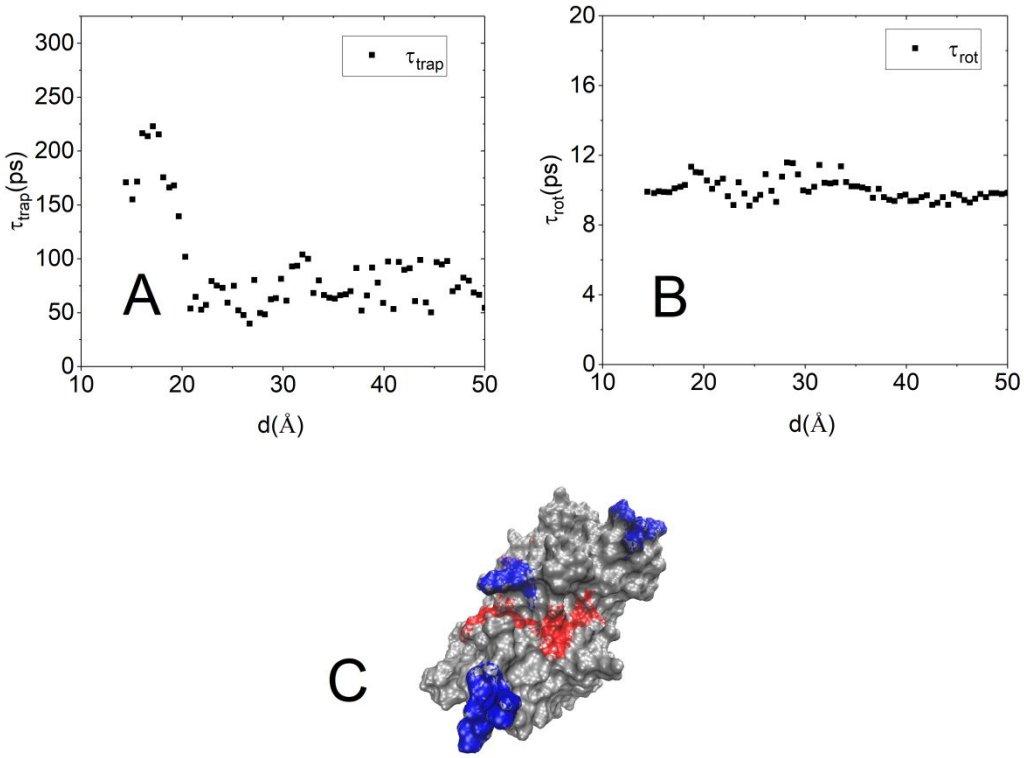

Figure 4. Spatial distribution of (A) τ_{trap} and (B) τ_{rot} of water molecules mapped to the nearby protein-surface residues, as a function of their distance from the center of mass of the protein. Data corresponds to the sample at h=4.0. (C) Protein-surface residues around which the water exhibits the top 10% longest values of τ_{trap} (highlighted in red), which constitue the peak at ~ d=17 Å (τ_{trap} >100ps) in A, and are mostly located at the clefs or concave spots on the protein surface. Details of the top 10 residues around which water molecules exhibit the slowest translation are shown in Table S2. In comparison, the residues around which the water exhibits top 10% smallest τ_{trap} are highlighted in blue, which are primarily distributed at the most exposed ridges of the biomolecules.

As revealed by Fig. 3B to C, the protein-surface effect can affect water translation up to the second hydration layer while limiting its influence on water rotation in the first layer. One would expect the water translation might be more correlated over space than its rotation. This is indeed confirmed by Fig. 5A, where we compared the spatial correlation of τ_{trap} with that of τ_{rot} of water molecules, which are mapped to the nearby protein-surface residues, defined as,

$$SC(r) = \left\langle \tau(\vec{r}_i) \cdot \tau(\vec{r}_j) \right\rangle, \tag{3}$$

where i and j are the index of the protein residues, $\vec{r}_i$ and $\vec{r}_j$ are the position vector of the center of mass of residue i and j, respectively, r is the distance between the two residues $r = \left| \vec{r}_i - \vec{r}_j \right|$ averaged over the simulation trajectory, and the bracket denotes averaging over all residue pairs at this distance. As illustrated by Fig. 5A, *SC(r)* of τ_{trap} decays much slower over distance as compared to that of τ_{rot}. *SC(r)* of τ_{trap} is significantly positive (~0.3) at r=6Å, while *SC(r)* of τ_{rot} approximates

0 at this distance. This demonstrates that the correlation of translational motions between water molecules significantly extends to the second nearest neighbors, while the interaction between water rotations is mostly limited within the nearest neighbors. Hence, the data indicates that water translations are more correlated over space. This may appear to be intuitively obvious and in fact has been mentioned before in Refs [45, 46], but to our knowledge it has not been previously demonstrated explicitly, as we show in Fig. 5A.

The observation of stronger spatial correlation between translational motions of protein-surface water might result from the following mechanism. The translational motion of a water molecule requires a neighboring site on the protein surface to be vacant for it to jump into, and the formation of this vacancy likely requires moving away a previously occupied water molecule. Hence, a water molecule is likely to be trapped for a longer time at a given site if the surrounding water molecules are in deep energy basins, leading to the spatial correlation of translational motions between adjacent water molecules. In contrast, the rotational motion of water molecules is relatively localized, and is thus less affected by such inter-water steric effect and only perturbed in the first hydration layer. To further illustrate this point, we performed MD simulations of the same protein at a series of lower hydration levels, h=0.4, 0.3, 0.2 and 0.1. Here, h=0.4 corresponds roughly to a single-layer coverage of water on the protein surface, and further decrease of h will lead to loose packing of water molecules, and thus alleviate the inter-water steric effect. As shown in Fig. 5B, decreasing h from 1.0 to 0.1 will increase the correlation coefficient between τ_{trap} and τ_{rot}, C_corr, defined in Eq. (4), from 0.023 to 0.151. This implies that the inter-water steric effect facilitates the decoupling between rotational and translational motions of the hydration water.

$$C\_corr = \frac{\left\langle \tau_{trap} * \tau_{rot} \right\rangle}{\sqrt{\left\langle \tau_{trap}^2 \right\rangle * \left\langle \tau_{rot}^2 \right\rangle}}, \tag{4}$$

where τ_{trap} and τ_{rot} are the translational and rotational characteristic times mapped to the same protein-surface residue at a given hydration level, respectively, and the $\langle\rangle$ bracket denotes the ensemble average.

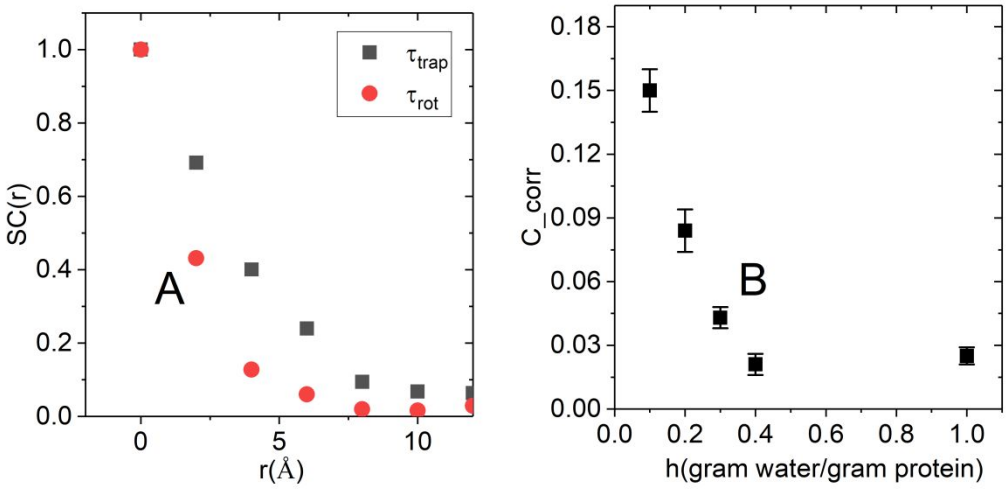

Figure 5. (A) The spatial correlation, *SC(r)*, as calculated from Eq. (3), of τ_{trap} and τ_{rot}, normalized by the value at r=0. To improve statistics, r is binned in every 2 Å. (B) The correlation coefficient, C_corr, as calculated from Eq. (4), between τ_{trap} and τ_{rot} at various low hydration levels.

The charge/polarity effect of the protein surface on dynamics of surrounding water molecules is also investigated. In Fig. 6, we compared τ_{trap} and τ_{rot} mapped at different types of residues on the protein surface: i.e., charged, polar and nonpolar amino acids. We found that the charged and polar residues slow down the dynamics of water much more significantly as compared to the non-polar residues. The effect is much more pronounced on water translation than its rotation.

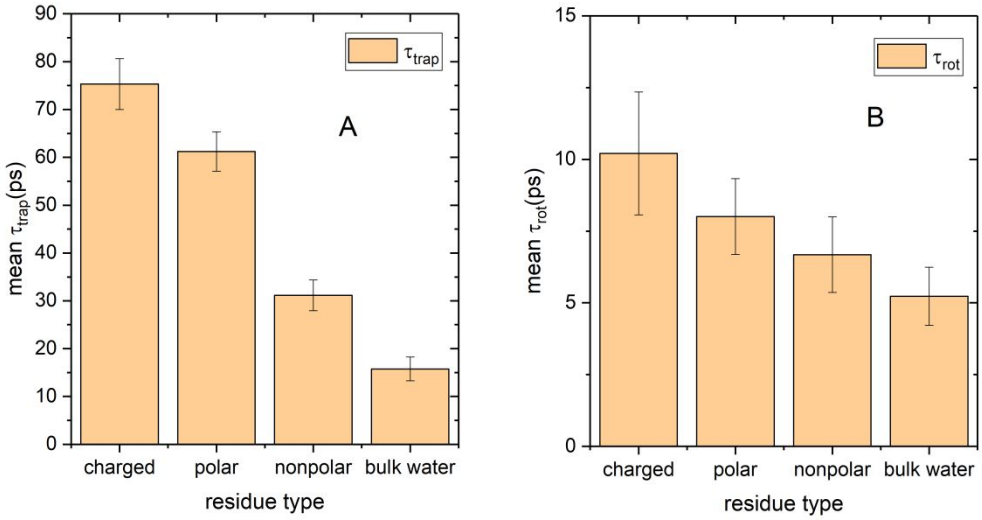

Figure 6. The mean values of τ_{trap} (A) and τ_{rot} (B) of water molecules around different types of residues.

To seek the connection between the dynamical decoupling in hydration water and the local flexibility in the protein, we calculated the ratio of τ_{trap}/τ_{rot} of water molecules nearby each protein residue and compared it to the root-mean-square fluctuation (RMSF) of the residue. Fig. 7A marks the protein residues which have the largest τ_{trap}/τ_{rot} (top 10%), i.e., the neighboring water presents the most decoupled translation and rotation. Meanwhile, Fig. 7B highlights the top 10% structurally most stable residues, which have the smallest RMSF and are found to be the key residues to form protein surface alpha helices and beta sheets. A strong overlap (~40%) is observed between these two types of residues (Fig. 7A and B). Such overlap indicates that water molecules around the stable protein residues likely exhibit the stronger translation-rotation decoupling, with translational motions severely constrained (Fig. 7C), while the rotational freedom remains approximately intact (Fig. 7D). This is further supported by a more thorough comparison between the RMSF and τ_{trap}/τ_{rot} for all protein residues in figure 7E, where most maxima (peaks) in τ_{trap}/τ_{rot} correspond to the minima in RMSF. Hence, the translation-rotation decoupling of hydration water could be connected to the local stability of the protein molecule. As described by Ref [9, 16-18], by losing substantial translational mobility, water molecules become part of the protein structure, which bridge the neighboring amino acids through hydrogen bonds or screen non-favored electrostatic interactions between nearby protein residues, and thus protect the local protein structure. Meanwhile, as proposed by Ref.[18], maintaining the rotational mobility can reduce the entropy cost to form these strongly trapped structural water molecules, which will decrease the free energy of the associated local protein structure, facilitating its stability. Hence, both restraining of the translational motion and

maintaining the rotational mobility of water molecules can contribute to the local stability of the protein molecule.

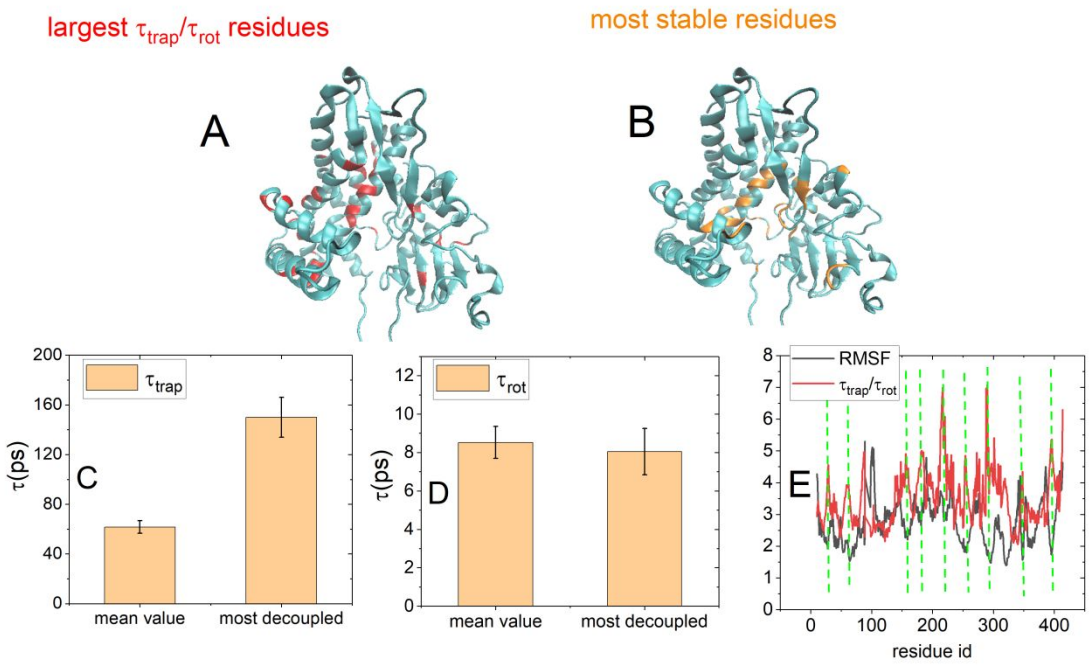

Figure 7. (A) Spatial distribution of protein residues with top 10% of largest ratio of τ_{trap}/τ_{rot} (marked in red), around which water molecules exhibit the greatest decoupling between rotation and translation. (B) Spatial distribution of the top 10% structurally most stable protein residues (marked in orange), which are characterized by the smallest RMSF. Comparison of (C) τ_{trap} and (D) τ_{rot} of water having the most decoupled dynamics (highlight red in (A)) with respect to those averaged over all surface water at h=4.0. (E) The relationship between RMSF and τ_{trap}/τ_{rot} of protein-surface residues. The dash green lines mark the correspondence between the peaks in τ_{trap}/τ_{rot} and the minima in RMSF.

Conclusion

In the present work, quasi-elastic neutron scattering measurements of water on a perdeuterated protein at well-controlled hydration levels, we found that the translation and rotational motions of water are slowed down and decoupled when reducing the level of hydration. Comparison with results from MD simulations suggest that the decoupling results from the fact that the water translations are highly restrained by the spatial confinement and charged/polar residues on the protein surface, and they are much more correlated over space as compared to the rotational motions. Furthermore, the water molecules with the more decoupled dynamics are often neighboring the structurally more stable protein residues, as restraining the translational motion and maintaining the rotational freedom of these water molecules might both contribute to the local stability of the biomolecule.

The translation-rotation decoupling in hydration water and its connection to the bio molecular stability discovered here could be general for a broad range of globular proteins, and suggest new perspective on the dynamics of hydration water as well as its biological role. However, the extent for such decoupling might depend on amino acid length, morphology and hydrophilic properties of the protein, which deserves further exploration.

Moreover, these findings can also rationalize the conflicting results reported by different experimental techniques on the amplitude and spatial range for the perturbed dynamics in hydration water. These techniques, including NMR, neutron scattering, dielectric spectroscopy, depolarized light scattering, 2D-infraed spectroscopy and THz spectroscopy, etc., probe distinct types of water motions, including rotation, translation, vibration, etc., and the measured time scale spans from femtoseconds to nanoseconds. The distinct dynamic processes measured on different time scales may be altered differently by the biomolecule, such as the translation-rotation decoupling revealed in the present work. In future, it will be highly desirable to apply one single experimental technique, e.g., neutron scattering, to characterize the dynamics of water in the same biological system over the whole femto-to-nanoseconds time window to explore how different types of water motions are affected by the bio macromolecules as well as their biological significance.

Associated content

Supporting information

Details of deuterated protein synthesis, neutron scattering experiment, MD simulations, fitting results and the calculation method can be obtained in supporting information.

Author Information

Corresponding author

*hongl3liang@sjtu.edu.cn

Author Contributions

The manuscript was written through contributions of all authors.

Notes

The authors declare no competing financial interest

Acknowledgements

The authors acknowledge NSF China 11974239, 31630002 and the Innovation Program of Shanghai Municipal Education Commission. The neutron scattering experiment on BASIS (SNS, ORNL) was supported by the Scientific User Facilities Division, Office of Basic Energy Sciences, U.S. Department of Energy. The authors acknowledge the Center for High Performance Computing at Shanghai Jiao Tong University for computing resources, and the student innovation center at Shanghai Jiao Tong University.

Reference

1. J. A. Rupley and G. Careri, *Advances in Protein Chemistry*, 1991, **41**, 37-172.
2. P. Ball, *Proceedings of the National Academy of Sciences*, 2017, **114**, 13327.
3. P. Ball, *Chemical Reviews*, 2008, **108**, 74-108.
4. P. W. Fenimore, H. Frauenfelder, B. H. McMahon and F. G. Parak, *Proceedings of the National Academy of Sciences*, 2002, **99**, 16047-16051.
5. D. Laage, T. Elsaesser and J. T. Hynes, *Chemical Reviews*, 2017, **117**, 10694-10725.

6. M. C. Bellissent-Funel, A. Hassanali, M. Havenith, R. Henchman, P. Pohl, F. Sterpone, D. Van Der Spoel, Y. Xu and A. E. Garcia, *Chemical Reviews*, 2016, **116**, 7673-7697.
7. P. K. Nandi and N. J. English, *The Journal of Physical Chemistry B*, 2016, **120**, 12031-12039.
8. M. S. Cheung, A. E. García and J. N. Onuchic, *Proceedings of the National Academy of Sciences*, 2002, **99**, 685-690.
9. B. Jayaram and T. Jain, *Annu. Rev. Biophys. Biomol. Struct.*, 2004, **33**, 343-361.
10. J. M. J. Swanson, C. M. Maupin, H. Chen, M. K. Petersen, J. Xu, Y. Wu and G. A. Voth, *The Journal of Physical Chemistry B*, 2007, **111**, 4300-4314.
11. Y. Levy and J. N. Onuchic, *Annu. Rev. Biophys. Biomol. Struct.*, 2006, **35**, 389-415.
12. Y. Harano and M. Kinoshita, *Chemical Physics Letters*, 2004, **399**, 342-348.
13. S. K. Pal and A. H. Zewail, *Chemical Reviews*, 2004, **104**, 2099-2124.
14. J. W. R. Schwabe, *Current Opinion in Structural Biology*, 1997, **7**, 126-134.
15. P. Ball, *Cellular And Molecular Biology-Paris-Wegmann-*, 2001, **47**, 717-720.
16. U. Langhorst, R. Loris, V. P. Denisov, J. Doumen, P. Roose, D. Maes, B. Halle and J. Steyaert, *Protein Science*, 1999, **8**, 722-730.
17. V. P. Denisov, K. Venu, J. Peters, H. D. Hörlein and B. Halle, *The Journal of Physical Chemistry B*, 1997, **101**, 9380-9389.
18. C. Mattos, *Trends in Biochemical Sciences*, 2002, **27**, 203-208.
19. V. Conti Nibali and M. Havenith, *Journal of the American Chemical Society*, 2014, **136**, 12800-12807.
20. S. Perticaroli, L. Comez, M. Paolantoni, P. Sassi, A. Morresi and D. Fioretto, *Journal of the American Chemical Society*, 2011, **133**, 12063-12068.
21. S. Perticaroli, G. Ehlers, C. B. Stanley, E. Mamontov, H. O'Neill, Q. Zhang, X. Cheng, D. A. A. Myles, J. Katsaras and J. D. Nickels, *Journal of the American Chemical Society*, 2017, **139**, 1098-1105.
22. G. Schirò, Y. Fichou, F.-X. Gallat, K. Wood, F. Gabel, M. Moulin, M. Härtlein, M. Heyden, J.-P. Colletier, A. Orecchini, A. Paciaroni, J. Wuttke, D. J. Tobias and M. Weik, *Nature Communications*, 2015, **6**, 6490.
23. J. T. King and K. J. Kubarych, *Journal of the American Chemical Society*, 2012, **134**, 18705-18712.
24. K. Yokoyama, T. Kamei, H. Minami and M. Suzuki, *The Journal of Physical Chemistry B*, 2001, **105**, 12622-12627.
25. D. S. Grebenkov, Y. A. Goddard, G. Diakova, J.-P. Korb and R. G. Bryant, *The Journal of Physical Chemistry B*, 2009, **113**, 13347-13356.
26. M. Heyden, D. J. Tobias and D. V. Matyushov, *The Journal of Chemical Physics*, 2012, **137**, 235103.
27. D. Zhong, S. K. Pal and A. H. Zewail, *Chemical Physics Letters*, 2011, **503**, 1-11.
28. C. Mattea, J. Qvist and B. Halle, *Biophysical Journal*, 2008, **95**, 2951-2963.
29. F. Persson, P. Söderhjelm and B. Halle, *The Journal of Chemical Physics*, 2018, **148**, 215103.
30. E. H. Grant, *Annals of the New York Academy of Sciences*, 1965, **125**, 418-427.
31. K. Meister, S. Ebbinghaus, Y. Xu, J. G. Duman, A. DeVries, M. Gruebele, D. M. Leitner and M. Havenith, *Proceedings of the National Academy of Sciences*, 2013, **110**, 1617.
32. J. Qvist, E. Persson, C. Mattea and B. Halle, *Faraday Discussions*, 2009, **141**, 131-144.
33. A. Frölich, F. Gabel, M. Jasnin, U. Lehnert, D. Oesterhelt, A. M. Stadler, M. Tehei, M. Weik,

K. Wood and G. Zaccai, *Faraday Discussions*, 2009, **141**, 117-130.

34. G. M. Cooper, R. E. Hausman and R. E. Hausman, *The cell: a molecular approach*, ASM press Washington, DC2000.
35. P. Tan, Y. Liang, Q. Xu, E. Mamontov, J. Li, X. Xing and L. Hong, *Physical Review Letters*, 2018, **120**, 248101.
36. L.-R. Zheng and L. Hong, *Chinese Journal of Polymer Science*, 2019, **37**, 1083-1091.
37. E. Mamontov and K. W. Herwig, *Review of Scientific Instruments*, 2011, **82**, 085109.
38. V. G. Sakai and A. Arbe, *Current Opinion in Colloid & Interface Science*, 2009, **14**, 381-390.
39. K. H. Andersen, D. Martín y Marero and M. J. Barlow, *Applied Physics A*, 2002, **74**, s237-s239.
40. L. E. Bove, S. Klotz, T. Strässle, M. Koza, J. Teixeira and A. M. Saitta, *Physical Review Letters*, 2013, **111**, 185901.
41. V. K. Peterson, in *Studying Kinetics with Neutrons: Prospects for Time-Resolved Neutron Scattering*, eds. G. Eckold, H. Schober and S. E. Nagler, Springer Berlin Heidelberg, Berlin, Heidelberg2010, pp. 19-75.
42. J. Teixeira, M. C. Bellissent-Funel, S. H. Chen and A. J. Dianoux, *Physical Review A*, 1985, **31**, 1913-1917.
43. P. Tan, J. Li and L. Hong, *Physica B: Condensed Matter*, 2019, **562**, 1-5.
44. S.-H. Chong and W. Kob, *Physical Review Letters*, 2009, **102**, 025702.
45. J. Qvist, C. Mattea, E. P. Sunde and B. Halle, *The Journal of Chemical Physics*, 2012, **136**, 204505.
46. J. Qvist, H. Schober and B. Halle, *The Journal of Chemical Physics*, 2011, **134**, 144508.